Relations of polarized scattering signatures observed by the TRMM Microwave Instrument with electrical processes in cloud systems

Catherine Prigent,[1] Eric Defer,[2] Juan R. Pardo,[3] Cindy Pearl,[4] William B. Rossow,[4] and Jean-Pierre Pinty[5]

Received 13 December 2004; accepted 27 January 2005; published 24 February 2005.

[1] The polarized scattering signatures observed in convective cloud systems with the Tropical Rainfall Measuring Mission (TRMM) Microwave Instrument are analyzed. In particular, and in contrast to the positive polarization difference (TbV-TbH > 0) observed when scattering by large ice particles is important, we also find a negative polarization difference. Radiative transfer simulations show that such a polarization difference can be explained by relatively large, mostly vertically oriented, non-spherical particles but not by horizontally or randomly oriented non-spherical particles. We establish a relationship between the occurrence of the negative polarization difference signature and electrical activity in the cloud using coincident observations by the Lightning Imaging Sensor also on board TRMM. The negative polarization difference is thus related to non-spherical particles that are mostly vertically oriented as revealed by the lightning activity. This result confirms that a careful analysis of passive microwave observations over clouds provides valuable information about the cloud ice phase. **Citation:** Prigent, C., E. Defer, J. R. Pardo, C. Pearl, W. B. Rossow, and J.-P. Pinty (2005), Relations of polarized scattering signatures observed by the TRMM Microwave Instrument with electrical processes in cloud systems, *Geophys. Res. Lett.*, *32*, L04810, doi:10.1029/2004GL022225.

1. Introduction

[2] Depending on the observed wavelength and on cloud and rain characteristics, the microwave radiation measured from a satellite can be affected by emission, absorption, and scattering. Emission/absorption by liquid water particles causes brightness temperature to increase over a radiatively cold background like the ocean. In contrast, scattering by the larger hydrometeors generally reduces the measured brightness temperature; large ice particles absorb much less than liquid particles so the scattering effect dominates when they are present in the upper portions of the cloud.

[3] The scattering signal measured by satellites at 85 GHz has been used to estimate precipitation and cloud ice content over land and ocean. Several studies have aimed at characterizing the convective activity from passive microwave scattering observations at 85 GHz [e.g., *Mohr et al.*, 1999] or relating the scattering signal to radar reflectivity or to electrical activity [e.g., *Nesbitt et al.*, 2000; *Toracinta et al.*, 2002]. The sensitivity of the scattering to the particle shape and orientation has already been shown from both model simulations, satellite observations, and ground based measurements [e.g., *Czekala et al.*, 2001]. *Prigent et al.* [2001] carefully characterized the scattering-related positive polarization difference (vertical minus horizontal) observed at 85 GHz with the Special Sensor Microwave/Imager (SSM/I) and interpreted it with the help of a radiative transfer model to show that the presence of mostly horizontally oriented non-spherical particles is needed within the stratiform anvil part of convective systems to explain the larger polarization magnitudes observed.

[4] In this study, the polarized scattering signatures observed with the Tropical Rainfall Measuring Mission (TRMM) Microwave Instrument (TMI) are analyzed. Compared to SSM/I, TMI provides significantly increased spatial resolution that makes it possible to resolve smaller structures associated with deep convection. In addition to positive polarization differences already observed in the scattering signal, negative polarization differences are also found (section 2). Using the same radiative transfer model, the negative polarization differences can be explained by mostly vertically oriented non-spherical particles (section 3). A relationship between the negative polarization difference and electrical activity in the cloud is shown, thanks to coincident observations from the Lightning Imaging Sensor (LIS) also on board the TRMM satellite (section 4). Section 5 concludes this study with special emphasis on the potential of passive microwave scattering signatures to characterize the convective processes in tropical cloud systems.

2. Observations of Polarized Scattering Signatures With TMI

[5] Since 1997, the TRMM satellite carries a suite of instruments designed for precipitation studies of the tropics [*Kummerow et al.*, 1998], including TMI and LIS that are used in this study. TMI measures the microwave radiation emitted by Earth and its atmosphere at five frequencies between 10 and 85 GHz in both vertical and horizontal polarizations (for most channels). It provides these measurements at a spatial resolution of 5×7 km at 85 GHz, compared to 15×13 km for the same channel on SSM/I.

[1]Laboratoire d'Etudes du Rayonnement et de la Matière en Astrophysique, Centre National de la Recherche Scientifique, Observatoire de Paris, France.
[2]Institute for Environmental Research, National Observatory of Athens, Athens, Greece.
[3]Instituto de Estructura de la Materia, Departamento de Astrofisica Molecular e Infrorroja, Consejo Superior de Investigaciones Científicas, Madrid, Spain.
[4]NASA/Goddard Institute for Space Studies, New York, New York, USA.
[5]Laboratoire d'Aérologie, Toulouse, France.

0094-8276/05/2004GL022225$05.00

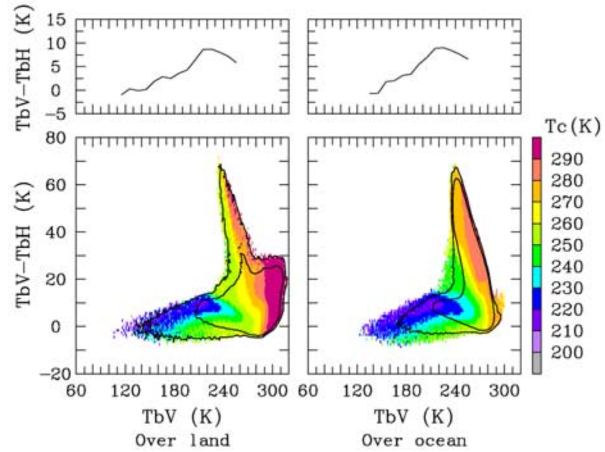

Figure 1. Scatterplots of the TMI brightness temperature polarization differences (TbV−TbH) versus the brightness temperatures in the vertical polarization (TbV), at 85 GHz for July 1998 over the tropics for cloudy pixels only. See text for more details.

[6] Similar to our previous study and based on the same data analysis technique [*Prigent et al.*, 2001], Figure 1 presents scatterplots of the TMI brightness temperature polarization differences (TbV - TbH) versus the brightness temperature at TbV at 85 GHz for July 1998. This is done for cloudy pixels only (cloudiness determined by the International Satellite Cloud Climatology Project (ISCCP) [*Rossow and Schiffer*, 1999] pixel closest in time and space). The ocean and land cases are treated separately. For each 1 K by 1 K box, the color indicates the mean cloud top temperature obtained by ISCCP (boxes with less than 10 observations are not included). Contours delimit regions where the pixel population in the boxes is larger than 0.001% and 0.0001% of the total population for the month. The emission and scattering regimes are easily recognizable, especially over ocean: against a cold background, thin clouds have rather low TbV with large polarization differences caused by the ocean surface but as cloud opacity increases, usually associated with a decrease of the cloud top temperature, TbV increases and the polarization difference decreases. In the scattering regime, most often observed for clouds with colder top temperatures, TbV decreases due to scattering by large ice particles and can achieve very low values, especially over land. The relative population of pixels with TbV $\sim \leq 220$ K is larger over land than over ocean. For each surface type, the upper panel in Figure 1 represents the most probable polarization difference at 85 GHz versus TbV. Limiting consideration to 60 K < TbV < 260 K and (TbV - TbH) < 15 K, we find that the mean polarization difference at first increases up to $\sim$7 K for TbV $\sim$ 220 K and then decreases below 0 K for TbV $\sim$ 140 K down to about ~ -2 K and ~ -1 K over land and ocean, respectively. At lower microwave frequencies, less scattering is observed, although the signal is again stronger over land than over ocean (not shown). Using the spatial standard deviation of the 85 GHz observations, we find that the larger positive polarization differences are associated with areas with lower spatial standard deviations (i.e., stratiform cloud regions as shown in our previous study), whereas the negative polarization differences are dominant in spatially heterogeneous regions (i.e., in deep convective regions).

[7] In the previous study, we examined the causes of the larger positive polarization differences observed in SSM/I measurements around TbV $\sim$ 220 K. A potential contribution of a polarized signal coming from the surface was ruled out and the signal was clearly related to the presence of cold-topped, optically thick clouds. Radiative transfer simulations demonstrated that the presence of large spherical particles can only generate positive polarization differences of the order of 2 K. Randomly oriented non-spherical particles cannot produce positive polarization differences as large as seen either. We showed that large positive polarization differences can only be explained by the presence of mostly horizontally oriented non-spherical particles. In the stratiform regions, forces on falling non-spherical particles are expected to align them horizontally, especially the largest precipitation-sized particles (the forces being size dependent).

[8] With SSM/I no negative polarization differences were observed, likely because these regions are too small scale to be resolved by the lower resolution of SSM/I. What cause the negative polarization differences observed with TMI? Could it be due to vertically oriented non-spherical particles in the convective cores of convective systems?

3. Radiative Transfer Calculations of Polarized Scattering

[9] To explore this explanation, the radiative transfer equation is solved for a plane-parallel atmosphere of gases and hydrometeors with the assumption that the hydrometeors are totally or at least azimuthally randomly oriented if they are not spherical. The far-field scattering by ensembles of totally or azimuthally randomly distributed spheroids is calculated using the method described by *Mishchenko* [1993, 2000]. The gas absorption is included according to *Pardo et al.* [2001]. Finally, the radiative transfer is performed following the Doubling-Adding method described by *Evans and Stephens* [1995]. For more details, see *Prigent et al.* [2001].

[10] A standard tropical atmosphere is assumed, similar to *Prigent et al.* [2001]: the only difference is that the monodisperse ice particles between 6.5 and 8.0 km are considered to be prolate spheroids with preferred vertical orientation instead of oblate spheroids with horizontal orientation as in the previous study. The particle orientation is considered to have its longest axis randomly distributed between $-\alpha_0$ and $+\alpha_0$ from the vertical. A refined weighting function in α could also be used to account for a steady oscillating behavior. Figure 2 shows the results of these simulations at 85 GHz: negative values of (TbV - TbH) are obtained with realistic prolate ice particles that are vertically oriented.

4. Particle Orientation and Electrical Activity

[11] Non-spherical particles that are large enough (>100 μm) with aspect ratios significantly different from unity are expected to align approximately horizontally as they fall. What mechanism could cause such particles to align vertically instead? Vertical orientation of particles in thunderstorms has already been suggested as early as 1965 [*Vonnegut*, 1965]. The first observations of electrically-

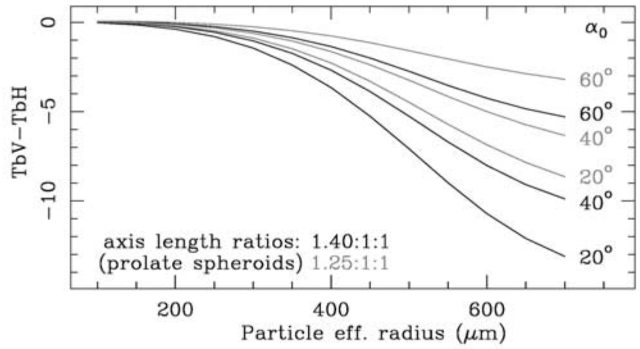

Figure 2. Sensitivity of the 85 GHz polarization difference to the orientation of the non-spherical ice particles as a function of particle size. The orientation of the particles is random within α_0 from the vertical axis.

induced particle alignment with ground radar were done by *Hendry and McCormick* [1976] and more recent developments [*Metcalf*, 1995; *Krehbiel et al.*, 1996] indicate the possibility of remotely characterizing the electrical fields in clouds by polarized ground radar measurements. Could the negative polarization differences observed by TMI in the scattering regime be related to electric fields?

[12] This hypothesis can be tested with the observations of LIS on the same TRMM platform. LIS senses and locates the radiation emitted by both cloud-to-ground and cloud-to-cloud flashes at 777 nm wavelength during day and night [*Christian et al.*, 2003]. It consists of a 128 $\times$ 128 CCD array with a time sampling of 2 ms coupled to wide-angle lens. LIS detection efficiency exceeds 90% [*Boccippio et al.*, 2002]. At the altitude of TRMM and for the periods studied here, LIS can observe a point on Earth within its field-of-view for about 80 s. Typically a flash is sensed by LIS as a succession of 2 ms samples (not necessarily continuous in time) with a given number of illuminated pixels providing a two-dimensional image of the flash extent. Within the reference 0.2° $\times$ 0.2° spatial grid box adopted in this study, all illuminated LIS pixels are considered along with their radiance. Radiance corresponds to the cloud-top for the range of LIS narrowband filter and is not from flash channels themselves but from multiple scattering processes within the cloud.

[13] Similar to Figure 1, Figure 3 shows the scatterplots of the (TbV - TbH) versus TbV at 85 GHz for July 1998 over land and ocean separately with the colors indicating the average percentage of flash detection with LIS for each 1 K by 1 K box. The scatterplots are limited to the cloudy pixels for which both LIS and TMI observations are available. Over land more than 50% of the cases with TbV below 180 K is associated with lightning detection and with (TbV - TbH) close to or below 0 K. Over ocean much less lightning is detected, confirming previous studies by *Toracinta et al.* [2002] and *Christian et al.* [2003].

[14] Figure 4 focuses on the strong scattering regime over land and presents histograms of the radiance index of the detected flashes for each 10 K interval of TbV and 3 K interval of (TbV - TbH) at 85 GHz for July and October 1998, January and April 1999. In each box the number of considered cases (when > 100) is indicated along with the percentage of pixels with lightning detection. For a given range of TbV, the percentage of pixels associated with lightning events increases with decreasing (more negative) polarization difference.

[15] The coincidence of LIS detections and low-to-negative polarization differences at 85 GHz from TMI in deep convective clouds (low TbV, low cloud top temperature, high optical thickness, not shown) is meaningful and appealing. The physical interpretation we offer involves a microphysical composition of the cores of deep convective systems containing a substantial amount of non-spherical graupels. The graupel is the key factor for promoting electrical activity, a high microwave scattering efficiency and negative polarization differences, all occurring in the same location as viewed from TRMM. Non-inductive charging mechanisms due to dry graupels colliding with small ice crystals and supercooled droplets are at the origin of the electrification of tropical convective clouds [*Takahashi*, 1979]. Lightning flashes follow when a polar electric field structure emerges due to the sedimentation of the charged hydrometeors. Although full understanding of electrical phenomena is not yet complete, the high correlation at cloud system scale between the occurrence of lightning flashes and graupel (as indicated by the microwave scattering signature) is consistent. In addition, recent radar observations at 95 GHz reported by *Wolde and Vali* [2001] show that dry graupels may lead to a slight negative polarization difference in radar reflectivity (Z). The shape of the graupel (prolate elongation or cone-like) and the preferential vertical orientation of the symmetry axis of these particles can explain this feature. Extension of this property to passive microwave radiometry, with Tb instead of Z, is straightforward. As a result, the simultaneous observation of a LIS signal and of a negative TbV-TbH at 85 GHz on TMI gives a reasonable indication of graupels.

5. Conclusion

[16] The negative polarization difference signature observed by TMI has been analyzed with the help of a radiative transfer model and coincident LIS lightning observations. The negative polarization difference is interpreted in terms of large, non-spherical mostly vertically oriented rimed particles to explain the electrical activity. The TMI spatial resolution at 85 GHz makes it possible to resolve the presence of vertically oriented graupels localized in small-areas where the strongest convective updrafts occur. This study confirms that a careful analysis of the passive micro-

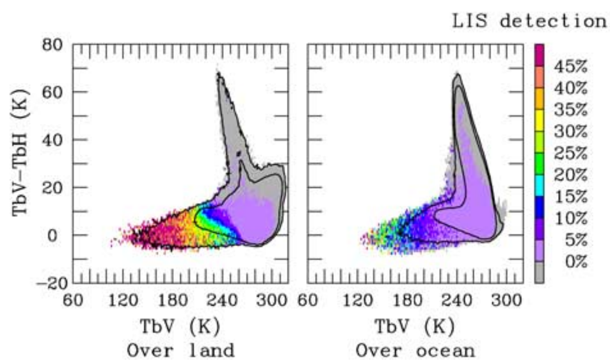

Figure 3. Same as Figure 1 but with the probability of the lightning detection in color.

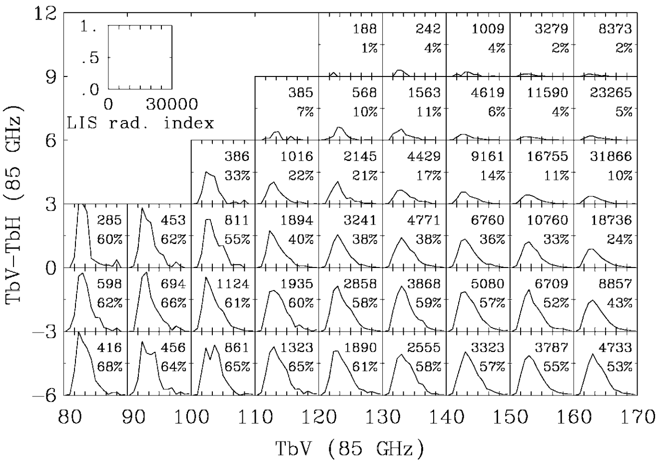

Figure 4. Histograms of the lightning radiance index for each 10 K TbV and 3 K TbV-TbH box at 85 GHz for four months over the continental tropics. For each box, number of cases is indicated along with the percentage of pixels with lightning detection.

wave observations, especially at higher spatial resolutions, is a very sensitive indicator of structures in tropical cloud systems, particularly concerning the ice particles and differences in behavior between the convective and stratiform parts of these systems. With adequate spatial resolution, passive microwave can also help characterize the relationship between cloud microphysical properties and electrical processes. This information can be used in the development and evaluation of realistic microphysical schemes in cloud models that also account for electrical activity.

[17] **Acknowledgment.** This study was supported, in part, by NASA funding for TRMM and ISCCP.

References

Boccippio, D. J., W. J. Koshak, and R. J. Blakeslee (2002), Performance assessment of the optical transient detector and lightning imaging sensor, part I: Predicted diurnal variability, *J. Atmos. Oceanic Technol.*, *19*, 1318–1332.

Christian, Hugh J., et al. (2003), Global frequency and distribution of lightning as observed from space by the Optical Transient Detector, *J. Geophys. Res.*, *108*(D1), 4005, doi:10.1029/2002JD002347.

Czekala, H., S. Crewell, A. Hornbostel, A. Schroth, C. Simmer, and A. Thiele (2001), Interpretation of polarization features in ground based microwave observations as caused by horizontally aligned oblate rain drops, *J. Appl. Meteorol.*, *40*, 1918–1932.

Evans, K. F., and G. L. Stephens (1995), Microwave radiative transfer through clouds composed of realistically shaped ice crystals, part II, Remote sensing of ice clouds, *J. Atmos. Sci.*, *52*, 2058–2072.

Hendry, A., and G. C. McCormick (1976), Radar observations of the alignment of precipitation particles by electrostatic fields in thunderstorms, *J. Geophys. Res.*, *81*, 5353–5357.

Krehbiel, P., T. Chen, S. McCrary, W. Rison, G. Gray, and M. Brook (1996), The use of dual channel circular-polarization radar observations for remotely sensing storm electrification, *Meteorol. Atmos. Phys.*, *59*, 65–82.

Kummerow, C., W. Barnes, T. Kozu, J. Shiue, and J. Simpson (1998), The Tropical Rainfall Measuring Mission (TRMM) sensor package, *J. Atmos. Oceanic Technol.*, *51*, 809–817.

Metcalf, J. I. (1995), Radar observations of the effect of changing orientations of hydrometeors in thunderstorms, *J. Appl. Meteorol.*, *34*, 757–772.

Mishchenko, M. I. (1993), Light scattering by size/shape distributions of randomly oriented axially symmetric particles of a size comparable to a wavelength, *Appl. Opt.*, *32*, 4652–4666.

Mishchenko, M. I. (2000), Calculation of the amplitude matrix for a nonspherical particle in a fixed orientation, *Appl. Opt.*, *39*, 1026–1031.

Mohr, K. I., J. S. Famiglietti, and E. J. Zipser (1999), The contribution to tropical rainfall with respect to convective system type, size, and intensity estimated from the 85 GHz ice scattering signature, *J. Appl. Meteorol.*, *38*, 596–606.

Nesbitt, S. W., E. J. Zipser, and D. J. Cecil (2000), A census of precipitation features in the Tropics using TRMM: Radar, ice scattering, and lightning observations, *J. Clim.*, *13*, 4087–4106.

Pardo, J. R., J. Cernicharo, and E. Serabyn (2001), Atmospheric Transmission at Microwaves (ATM): An Improved Model for mm/submm applications, *IEEE Trans. Geosci. Remote Sens.*, *49*, 1683–1694.

Prigent, C., J. R. Pardo, M. I. Mishchenko, and W. B. Rossow (2001), Microwave polarized scattering signatures in clouds: SSM/I observations interpreted with radiative transfer simulations, *J. Geophys. Res.*, *106*, 28,243–28,258.

Rossow, W. B., and R. A. Schiffer (1999), Advances in understanding clouds from ISCCP, *Bull. Am. Meteorol. Soc.*, *80*, 2261–2287.

Takahashi, T. (1979), Riming electrification as a charge generation mechanism in thunderstorms, *J. Atmos. Sci.*, *36*, 2236–2258.

Toracinta, E. R., D. J. Cecil, E. J. Zipser, and S. W. Nesbitt (2002), Radar, passive microwave, and lightning characteristics of precipitating systems in the tropics, *Mon. Weather Rev.*, *130*, 802–824.

Vonnegut, B. (1965), Orientation of ice crystals in the electric fields of a thunderstorm, *Weather*, *20*, 310–312.

Wolde, M., and G. Vali (2001), Polarimetric signatures from ice crystals observed at 95 GHz in winter clouds. Part I: Dependence on crystal form, *J. Atmos. Sci.*, *58*, 828–841.

E. Defer, Institute for Environmental Research, National Observatory of Athens, P.O. Box 20048, Thissio, GR-11810 Athens, Greece.

J. R. Pardo, Instituto de Estructura de la Materia, Departamento de Astrofisica Molecular e Infrorroja, Consejo Superior de Investigaciones Científicas, E-28006 Madrid, Spain.

C. Pearl and W. B. Rossow, NASA/Goddard Institute for Space Studies, New York, NY 10025, USA.

J.-P. Pinty, Laboratoire d'Aérologie, Toulouse, France.

C. Prigent, Laboratoire d'Etudes du Rayonnement et de la Matière en Astrophysique, CNRS, Observatoire de Paris, 61, avenue de l'Observatoire, F-75014 Paris, France. (catherine.prigent@obspm.fr)